27th ABCM International Congress of Mechanical Engineering
December 04-08, 2023, Florianópolis-SC, Brazil

COB-2023-1276
INTEGRATION OF SOLAR-ASSISTED COOLING SYSTEM AND HEAT PUMPS FOR INDUSTRIAL APPLICATIONS

Lorena Barros Guimarães
Emmanuel Damilano Dutra
Universidade Federal de Pernambuco, Cidade Universitária, Recife – PE, 50740-540.
lorena.bguimaraes@ufpe.br
emmanuel.dutra@ufpe.br

Deivson Cesar Silva Sales
Luis Arturo Gómez-Malagón
Instituto de Inovação Tecnológica da Universidade de Pernambuco, Várzea, Recife - PE, 50950-050.
deivsonsales@poli.br
lagomezma@poli.br

Abstract. *Steam and cooled water are utilities in the industrial sector that can be supplied by renewable energies. In this way, the application of a Solar Energy Assisted Heat Pump (SAHP) and a Solar Energy Assisted Adsorption Cooling System (SAACS) can be exploited to achieve this purpose, respectively. The thermal modeling of these systems was performed using the TRNSYS software, considering a HP operating with R600a and an ACS using silica-gel/water. The study evaluates the impact of condensation temperature (T_{cond}) on key performance metrics such as coefficient of performance (COP), solar field size given by the solar collector area (A_c) and solar utilization factor (SUF). The results indicate that SUF values decrease with increasing A_c, HP COP decreases with increasing T_{cond}, while ACS COP remains constant. The electrical power demands for SAHP and SAACS were 5.57kW and 0.55kW considering heating capacity of 11.58kW and cooling capacity of 6.5kW, respectively. From the environmental point of view, the proposed system proves to be advantageous, reducing the Global Warming Potential (GWP) by 72.2%, 82.4% and 56.2% compared to Liquefied Petroleum Gas (LPG) and firewood boiler combined with a cooling system and a double cascade HP (DCHP), respectively.*

Keywords: *so1ar energy, heat pumps, adsorption chiller, TRNSYS.*

1. INTRODUCTION

In industrial processes, steam and cold-water demands are usually supplied by boilers and compression HP, respectively. The boilers' energy source typically comes from fossil fuels such as firewood or Liquefied Petroleum Gas (LPG), which are not environmentally friendly or can be expensive depending on the energy market (IPCC, 2023). On the other hand, a HP uses a vapor compression cycle with refrigerant fluid that must fulfill the requirement of environmental protocols, such as Montreal's protocol for the use of fluorocarbon gases (IDEC, 2022). These characteristics associated with the energy source and technology are barriers to the sustainable development of the generation of process heat in the industry. An alternative to mitigate negative impacts in the generation of process heat is the use of renewable energy sources. At this point, solar energy can be introduced into the energetic matrix reducing the consumption of conventional energy sources.

There are different approaches to produce steam, such as high-temperature heat pumps (HTHP), solar parabolic trough collectors (Saini et.al., 2023) and photothermal materials with strong optical absorption (Lin et. al., 2019). In particular, HTHP has attracted the attention of the industrial sector due to the possibility of using the waste heat in the range of 60°C to 99°C which corresponds to 56.3% of the estimated total industrial waste heat (Kang, et al., 2017). It is important to observe that the range of temperatures for waste heat matches the temperature range of hot water obtained using low-temperature solar thermal systems, indicating that solar energy can boost HTHP application. Different configurations of HTHP are studied in the literature, such as single-stage, multi-stage system, cascade, and hybrid (Jiang et al, 2022). Between them, the double cascade heat pumps (DCHP) have been shown to be an alternative to generate steam from heat sources at relatively low temperatures (Lu, et al., 2022) (Mateu-Royo, et al., 2021) (Wu, et al.,2021) (Guimarães et. al., 2022). It means that coupling solar thermal systems in the intermediate exchanger of a DCHP can be an option to generate steam with low electric energy consumption. On the other hand, cold water can be also obtained using an absorption chiller driven by waste heat (Haywood, et al., 2012) (Dadpour, et. al., 2022) (Liu, et al. 2020). As a result, this technology becomes a viable candidate to be powered by solar thermal systems as well.

Thermal systems assisted by solar energy are explored in the literature to obtain cold and hot water. For example, cold water can be obtained using hot water from a solar thermal system to heat the generator of a single absorption chiller (Alhamer, et. al., 2016) or the adsorber of an adsorption/vapor compression refrigeration system (Gado, et. al., 2021) (Gado, et. al., 2022). Also, hot water can be obtained using solar energy to evaporate the refrigerant fluid of a HP to increase the condenser temperature (Hawlader et. al., 2001). Furthermore, solar energy can be used to produce hot and cold water for space heating and cooling depending on the season (winter or summer) using an integrated system of a HP and adsorption chiller fed by hot water from a solar thermal system (Calise, et. al., 2017). Besides, sensible heat thermal storage integrated with these poly-generation systems can be employed in the air conditioning systems of buildings to be operated according to energy price (Chen, et. al., 2020).

For industrial applications, there are some challenges associated with the hot and cold-water supply. For example, for the food processing industry are the high hot water temperatures, the overlapping of cooling and heating demands, and also the cost of Photovoltaic/Thermal (PVT) systems (Herrando et.al., 2021). Also, there is a need to analyze the dynamical operation of the system under variable conditions to minimize the excess of energy production and maximize the annual life-cycle cost savings (Hiben et. al., 2023). Therefore, this work aims to analyze a SAHP and a SAACS to produce steam and cold water for an industrial application.

Considering these aspects, the present work studied the performance of COP and SUF on A_C under different HP condensation temperatures, and also, the environmental impact was determined by the GWP comparing the conventional and the proposed system to meet the demands of refrigeration and steam generation in the small industrial sector.

2. METHODOLOGY

An SAHP and a SAACS were modeled to meet the cooling and heating demands of an industrial application associated with the temperature change of 0.4 m³/h of water from room temperature to 6ºC, and steam generation at atmospheric pressure with volumetric flow between 0.015 – 0.025 m³/h. The processes are not simultaneous, which means that initially the generation of steam is required followed by the cooling process (Dumbliauskaite et. al., 2010) (Liu et. al., 2017) (Masera et. al., 2023). For the proposed process, steam is required for 1h, followed by the cooling process for 40 min. An interval of 30 min between the heating and cooling processes was considered. Then, in order to optimize the use of solar radiation, the process is considered to work between 11:00 a.m to 1:10 p.m for the whole year.

The proposed system is a solar thermal system composed of a field of flat plate collectors coupled with the storage tank of hot water, which will supply energy to the evaporator of a single HP and also, the generator of an adsorption chiller. For the HP, the R600a refrigerant fluid was employed due to its capacity to achieve high temperatures in a high-pressure cycle (Guimarães et. al., 2022). For the adsorption cooling system, a pair of silica-gel/water was chosen because the regeneration temperature is low (55°C – 100°C) and can achieve low outlet water temperatures (Alahmer et. al., 2016). Also, the R600a and the silica-gel have a low environmental impact when they are released to the environment (Embraco, 2020) (Lu et. al., 2011) (Denzinger et. al., 2021). The diagram of the proposed system is shown in Figure 1.

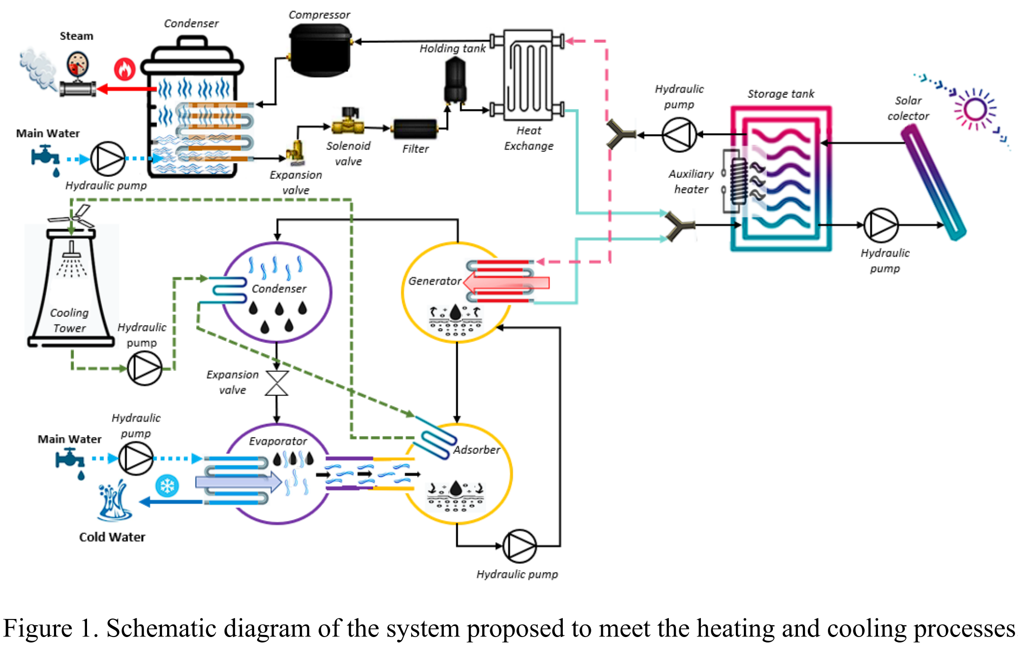

Figure 1. Schematic diagram of the system proposed to meet the heating and cooling processes.

The system was modeled using the Transient System Simulation Software (TRNSYS®), which is widely used to simulate the thermal behavior of thermal systems such as solar thermal collectors, HP, and adsorption chillers (Li et. al., 2014) (Bawazir et. al., 2022) (Younes et. al., 2023). The flow diagram of the proposed system is shown in Figure 2. The system is formed by blocks called of *types* which are connected between them to address the information. Table 1 presents a summary of the components of the proposed system and the associated elements used in the simulation tool.

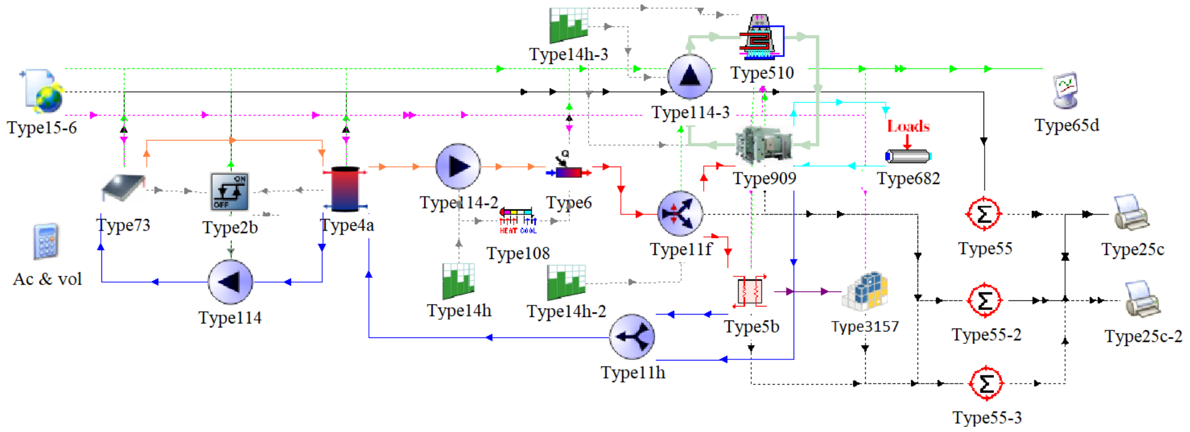

Figure 2. System layout proposed in TRNSYS®.

Table 1. List of the components (*Types*) used in the simulation on TRNSYS® with important parameters and inputs.

System Component	TRNSYS Element	Description
Weather data reading and processing	Type 15-6	Meteonorm® file (TMY2) for the location and conditions of tropical dry savana climate (MinData, 2023).
Flat-plate solar collector	Type 73	Collector efficiency factor 0.68, the loss coefficient for the bottom and edges 5.97 kJ/h.m².K, the slope is 18° and the azimuth angle is 0°.
Water pump	Type 114	Type 114 (recirculation); Type 114-2 (main feed); Type 114-3 (cooling tower circuit). Rated flow rate of 50 kg/h.m², 400 kg/h and 3300 kg/h, respectively.
Controller	Type 2b	The controller will remain off until the monitored temperature falls below the high limit cut-out temperature (80°C).
Storage water tank	Type 4a	Volume of the storage tank is 75liters/m².
Forcing function	Type 14h	Type 14h (whole process: 2h10min); Type 14h-2 (heating process: 1h); Type 14h-3 (cooling process: 40min). Value of the function (0 for OFF and 1 for ON) over the desired period of time.
Auxiliary heater	Type 6	Desired temperature is set at 85°C for the regeneration temperature of silica-gel maximum heating rate is 13 kW.
Thermostat	Type 108	Triggered when the temperature being monitored is below the desired (85°C) is the one at which the auxiliary heating is commanded.
Flow diverter valve	Type 11f	The input control signal defines the position of a damper by controlling the ratio of valve opening to each fluid outlet (0 trigger only the cooling process and 1 trigger only the heating process).
Adsorption chiller	Type 909	The conventional adsorption cooling system using silica-gel/water pair. Rated capacity is 10 kW and chilled water setpoint temperature is 6°C.
Flow stream thermal load	Type 682	Flow stream thermal load to the cooling process 6.5 kW.
Cooling tower	Type 510	For the condenser. Rated fan power is 1.5 kW.
Counter flow heat exchanger	Type 5b	The load side flow rate and the overall heat transfer coefficient of the exchanger are determined according to the integration of compression HP modeling in Python®, of the inlet temperature and the flow rate from the source side.
Compression HP	Type 3157	The component calls a Python® module implemented in a file located in the same directory as the TRNSYS® input file at the runtime (Bernier et. al., 2022). This module represents the modeling of the compression HP system (Guimarães et. al., 2022).
Flow mixer valve	Type 11h	In this work this valve was used to ensure the output of a single flow from two fluid circuits with different inputs and drive times. It can also be used to mix two inlet liquid streams into a single outflow.

Periodic integrator	Type 55	Type 55 (whole process: 2h10min); Type 55-2 (cooling process: 40min); Type 55-3 (heating process: 1h). This component calculates the mean of a series of inputs over a range of time periods specified by the user. In addition, the component calculates the sum of an input over the same specified range time (11:00 AM to 1:10 PM).
Printer	Type 25c	Type 25c (temperature); Type 25c-2 (energy). This component is used to print output variables selected from the system at specified intervals of time.
Online plotter	Type 65d	This component is used to display selected system variables as the simulation progresses. Also, it is highly recommended and widely used since it provides information about the variables and allows users to immediately see if the system is not performing as desired.

2.1 Metric of performance

The system's performance was evaluated by performance indicators. The Coefficient of Performance (COP) of the system is defined as the ratio between the useful energy used in the process and the energy employed to perform the process. The COP of the compression heat pump (COP_{hp}) and the COP of the adsorption chiller (COP_c) were determined during the period of the heating and cooling processes, respectively.

In particular, the COP_c is defined as the relationship between the cooling load and the sum of the heat absorbed by the generator and the total work performed by the hydraulic pump. However, generally, the electricity consumption of the pump in the adsorption chiller is extremely low and can be overlooked. Therefore, the COP_c was determined according to Eq. (1) (Bellos et. al., 2016) (Cabrera et. al., 2013):

$$\mathrm{COP}_c = \frac{\dot{\mathrm{Q}}_{ref}}{\dot{\mathrm{Q}}_g+\dot{\mathrm{W}}_c} \cong \frac{\dot{\mathrm{Q}}_{ref}}{\dot{\mathrm{Q}}_g}, \tag{1}$$

where $\dot{\mathrm{Q}}_{ref}$ is the cooling thermal load (kW), $\dot{\mathrm{Q}}_g$ is the amount of heat absorbed by the chiller generator (kW) and $\dot{\mathrm{W}}_c$ is the total work performed by the pump (kW).

The COP_{hp} is defined as the relationship between the heat released by the condenser and the total work performed by the compressor according to Eq. (2):

$$\mathrm{COP}_{hp} = \frac{\dot{\mathrm{Q}}_{cond}}{\dot{\mathrm{W}}_{hp}}, \tag{2}$$

where $\dot{\mathrm{Q}}_{cond}$ is the amount of heat released by the HP condenser (kW) and $\dot{\mathrm{W}}_{hp}$ is the total work performed by the compressor (kW).

For the solar thermal system, it is verified that the amount of energy delivered by the system is intrinsically dependent on the solar collection area. In this way, the solar fraction (F_s) is defined as the relationship between the amount of useful energy provided by the solar system and the total energy required to carry out the entire process (heating + cooling). Then, the solar fraction is defined by Eq. (3):

$$\mathrm{F}_s = \frac{\dot{\mathrm{Q}}_s}{\dot{\mathrm{Q}}_s+\dot{\mathrm{Q}}_{aux}}, \tag{3}$$

where $\dot{\mathrm{Q}}_s$ is the amount of useful thermal energy produced by the flat plate solar collector (kW) and $\dot{\mathrm{Q}}_{aux}$ is the heat generated by the auxiliary heater (kW).

For the proposed system, the amount of heat generated by the auxiliary heater is used as energy supplementation to regeneration temperature requirement for the adsorption chiller and also the temperature of the intermediate exchanger of the HP. So, the hot water produced by the flat plate solar collector stored in the thermal accumulation tank serves as preheated water for the adsorption system and the compression heat pump evaporator. Thus, it is verified that the collector can produce an average thermal energy whose value varies with the change in solar irradiance throughout the day.

The generation of energy delivered by the auxiliary heater is added to the energy delivered by the hot water storage tank to achieve the heat demand of the process. The amount of energy delivered by the auxiliary heater increases at the beginning of the day because the temperature of the water supplied by the storage tank is much lower than the necessary temperature (85°C) for the chiller. In the afternoon, the temperature delivered by the hot water storage tank is almost constant.

Due to the intermittency of solar thermal energy generation and the need to describe the performance of the component throughout the year, a Solar Utilization Factor (SUF) was established. This factor involves the conversion efficiency of solar energy into its cooling and heating capacity for steam generation, being defined as the relationship between the amount of useful thermal energy provided by the heating or cooling systems and the useful energy delivered by the solar thermal system throughout the year according to Eq. (4):

$$SUF = \frac{\int_0^{8760} \dot{Q}_{ref} \cdot dt + \int_0^{8760} \dot{Q}_{cond} \cdot dt}{A_c \cdot \int_0^{8760} H_t \cdot dt}, \quad (4)$$

where H_t is the overall irradiance in the collector surface plane (kWh/m²) and A_c is the gross collection area (m²).

2.2 Global warming potential assessment

The analysis of the environmental impacts, related to the process of generating steam and cooled water for industrial use resulting from the replacement of conventional equipment present in the sector by the hybrid system proposed in this study, was carried out through a comparative approach using the Life Cycle Assessment (LCA) method. This method is indicated to evaluate the impacts related to all stages, from the extraction of the raw material to the consumption or reuse of a resource linked to a process or product (ABNT ISO/NBR 14040-14044, 2009).

In this study, the Ecoinvent® database was used, and the chosen model was the "Allocation at the point of substitution (APOS)". The analysis method selected was the ReCiPe 2016 Hierarchist (Huijbregts et al., 2017) and the GWP is given in kg of $CO_{2(eq)}$/kWh.

The impact of the use of SAHP in meeting the thermal demand for heating is determined by the GWPs for conventional steam generation systems (boilers driven with LPG and firewood). The impact of the use of SAACS in meeting the thermal demand for refrigeration is determined by the GWP of a conventional compression cooling system to provide the supply of cooled water. For comparison, it was also included the GWP with the simultaneous attendance of the thermal demands through the use of a DCHP (Guimarães et. al., 2022).

Thus, the GWP for each process was obtained by the product between the consumption of thermal or electrical energy (in kWh) and the impact factor obtained from the database. In relation to the refrigerants used in SAHP, DCHP and conventional refrigeration systems, the value of the amount of $CO_{2(eq)}$ was obtained by multiplying the mass and the specific GWP of the fluid.

3. RESULTS AND DISCUSSION

This section presents the performance analysis of the proposed system. It was analyzed under optimized conditions of COP and SUF under different HP condensation temperatures established by Guimarães et. al. (2022). The parameters related to the solar resource were evaluated according to the collection area. In addition, at the end of this section, the GWP related environmental impact for this hybrid system was assessed comparing them to conventional refrigeration and steam generation methods.

3.1 Simulation analysis of the system

The reference system analyzed in this study is based on a quasi-static simulation strategy, which consists of the use of hourly average data of 3 consecutive days that are able to represent the significant characteristics of each month and illustrate a forecast of its operational performance. The representative days selected to compose this analysis are 01, 02 and 03 January (from 0 h to 72 h). In Figure 3 is shown the main temperatures of the system for the selected days, in which its operation is outlined.

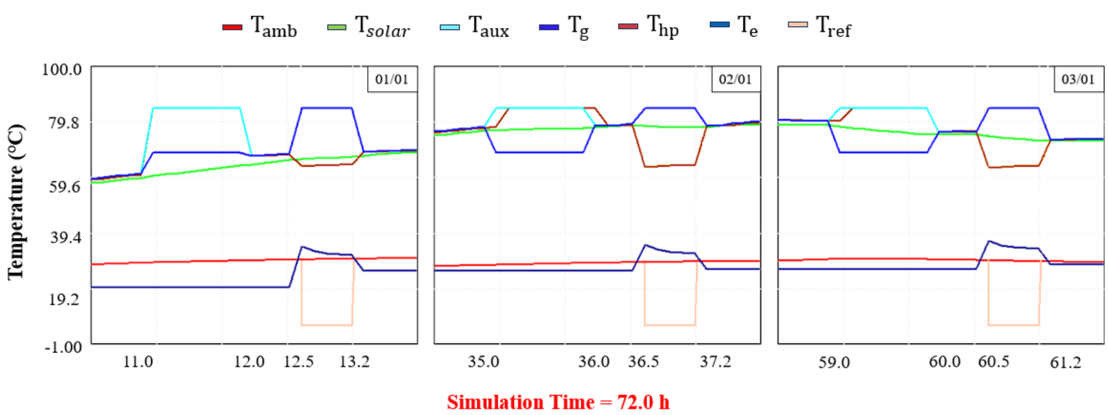

Figure 3. Temperature profile on time during three consecutive days.

Until 11:00 a.m. there is no demand for either heating or cooling, then, the solar thermal system line acts only for recirculation in order to raise the water temperature from the ambient (T_{amb}) to the solar storage (T_{solar}) temperatures. For the day 01/01, for example, we can observe that the water temperature is increased from ambient temperature to 59.7°C. The heating process by the HP begins at 11:00 a.m. and provides steam for 1 hour. Thus, the operation of the controllers that manage the main circuit feed pump (Type 114-2), the flow diverter valve (Type 11f) and the auxiliary heater (Type 6). At this stage, the water has its temperature increased by the auxiliary heater (T_{aux}), starting from T_{solar} until it reaches the level of 85°C, which is the desired inlet temperature for both the intermediate exchanger (T_{hp}) and the generator of the adsorption system (T_g). At noon the process is interrupted for approximately 30 min. It can be observed that T_{hp} decreases, as Types 114-2, 11f and 6 are turned off. Soon after (12:30 pm) the cooling process begins, in which the activation of the feed pump of the cooling tower circuit (Type 114-3), the tower hood (Type 510) and the adsorption chiller pump (Type 909) is evidenced. The last process takes place for about 40 min and soon after the system is shut down. In this step, Types 114-2, 11f and 6 are triggered again in order to meet T_g. In the chiller system, the cooling tower (T_e) is responsible for lowering the water temperature to meet the operating conditions in terms of condenser and adsorber temperature (~20°C). Thus, water has its temperature variation in this circuit around 15°C (35°C - 20°C). During the 40 min of cooling process, the temperature of the process water is lowered by the chiller (T_{ref}), starting from T_{amb} until it reaches the level of 6°C, which is the desired output temperature. The energy flows of the system can also be used to explain the dynamic behavior of the proposed system. Figure 4 shows the trends in energy flows.

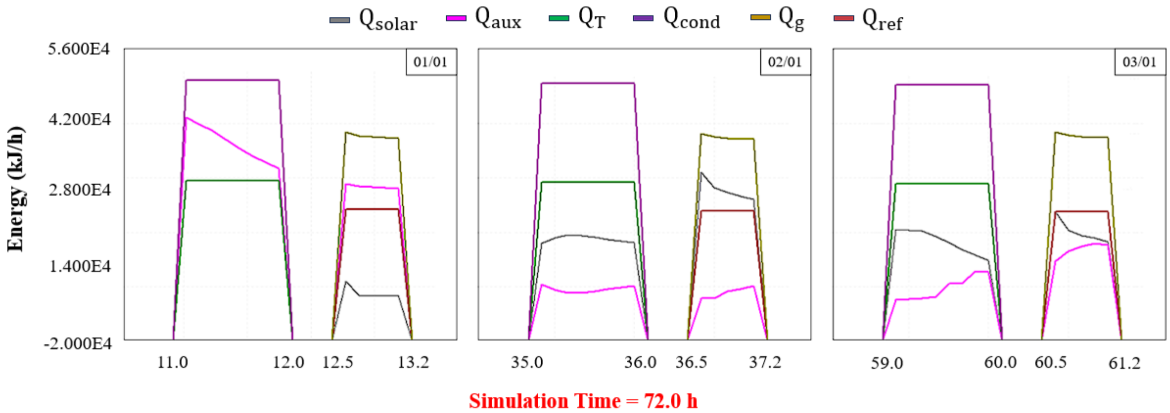

Figure 4. Heat profile on time during three consecutive days.

Solar radiation significantly affects the heat profiles produced by the solar thermal field, since the production of useful energy is directly related to radiation incident under its surface. From Figure 4, simulations for three days showed the complementarity of the energy for auxiliary and solar thermal systems. During the first part of the day, the thermal energy produced by the collectors is fully supplied to HP. Then, during the remaining hours of the day, solar energy provides energy to the adsorption chiller. On January 1st it was observed that in the period of 11:00 am to noon, there was little incidence of radiation, so the thermal heating load was strongly assisted by the auxiliary heater (Q_{aux}). This energy demand is necessary to meet the 85°C threshold in both the intermediate heat exchanger (Q_T = 28,548 kJ/h) and the adsorption chiller generator (Q_g = 36,000 kJ/h). After noon, it was observed that there was an increase in the amount of useful energy that comes from the solar thermal system (Q_{solar} = 8,040 kJ/h), so that it contributed with 22.3% in the fulfillment of the thermal load for the generator of the adsorption chiller. On January 2nd and 3rd, the opposite behavior was observed due to the high contribution of the energy stored in the hot water tank. For the heating system, Q_{solar} contributed 19,042 kJ/h (66.7%) and 18,534 kJ/h (64.9%), respectively. For the cooling system, Q_{solar} contributed with 26,473 kJ/h (73.5%) and 19,204 kJ/h (53.3%), respectively.

Thus, in order to establish an optimized performance condition, that is, the best possible COP for the proposed system, a relationship can be established between the fraction of available useful energy provided by the solar thermal system on the collection area for each compression HP condensation temperature, as shown in Figure 5. From it, it is observed that there was no significant difference between the solar fractions and the SUF values obtained through the variation of T_{cond} as the size of the solar field increases. Thus, it is verified that increasing the solar collector area, the F_S increases and the SUF decreases (Chen et. al., 2019).

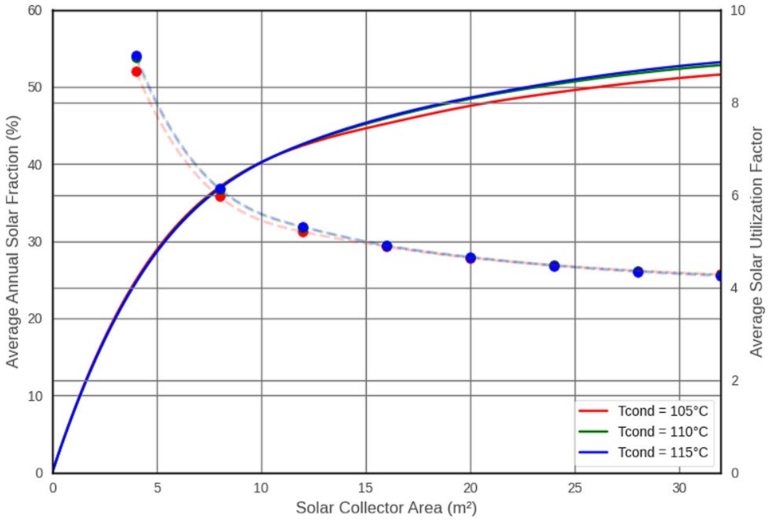

Figure 5. Average annual solar fraction and average solar utilization factor on collector area for different T_{cond} (105 °C, 110 °C and 115 °C).

Figure 6 shows the annual COP_{hp} for steam generation under different T_{cond}. It was observed that the COP_{hp} decreases as the condensation temperature of the HP cycle increases. This fact is due to the variation in the inlet power of the compressor, as a consequence of the variation of the refrigerant mass flow and its heating capacity. The maximum COP_{HP} value was at a condensation temperature of 105 °C, whose compressor input power obtained was 5.57 kW, with an efficiency of 39.3%, for the HP cycle. The mass flow of R600a required to the process was 0.049 kg/s, generating a heating capacity of 11.58 kW, and providing steam for a volumetric flow of 0.015 m³/h.

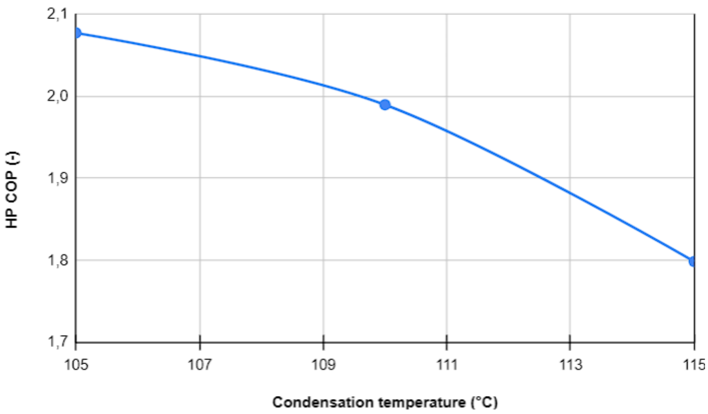

Figure 6. Coefficient of performance on condensation temperature for the HP.

In addition, the average annual COP_c was 0.41. It was obtained considering a water volumetric flow of 0.4 m³/h, with a thermal flow of 6.5 kW, whose hydraulic pump consumption is 0.55 kW. Similar values for the COP_c are reported in the literature [0.2 – 0.42] (Najeh et. al., 2016).

3.2 Enviromental analysis of the hybrid sytem

The environmental impact related to the GWP of each system is presented in Table 2. For calculation purposes, a mass of 1 kg was estimated for the refrigerant R600a for the hybrid system. This mass value was also considered for the low (with R134a) and high (with R600a) cycle of the DCHP presented by Guimarães et. al. (2022). It was compared with the conventional cooling system (with only R134a). The GWP of R134a and R600a over 100 years is given by 1430 and 4, respectively. Both fluids have Ozone Depletion Potential (ODP) equal to zero.

For the adsorption chiller, the gel-water silica pair has GWP and ODP equal to zero. For the conventional refrigeration system, power of 1.5 kW was considered to drive the compressor. This power value was estimated based on typical commercial values of condensing units that meet the cooling capacity required for cold water supply (4,124.2 kCal/h) (Guimarães et. al, 2022).

The annual consumption values of conventional systems were estimated based on the typical efficiency values of the boilers (LPG = 30%; firewood = 70%) (Jugjai and Rungsimuntuchart, 2002) (Chandrasekaran, 2011), and the amount of heat flow required to heating demands of the industrial sector analyzed (11.58 kW). Thus, to meet a heat flow of 11.58 kW using LPG, it is necessary for the burner to consume 38.6 kW (11.58/0.3) in 1 h for 21 days per month in 1 year.

On the other hand, the annual consumption value using wood heaters was estimated based on the Lower Calorific Value (LCV) of the firewood (LCV_{wood} = 2400 kCal/kg) (Alfa Laval Aalborg, 2022), the amount of fuel consumed to meet the demands of the industrial sector analyzed (M_{wood} = 15 kg) and the duration of the heating time in 1h with only one operation per day in a year.

The consumption value of DCHP developed by Guimarães et.al. (2022) was defined based on the sum of the values of the compressor input powers in each cycle (3.04 kW + 5.57 kW). In this case, the authors considered the operating time of 2 h, with only one operation per day, in one year, to meet both processes.

For the hybrid system proposed in this study, the value of the electrical consumption was defined from the values of the HP compressor power (5.57 kW) and the ACS hydraulic pump (0.55 kW), considering that the systems do not operate simultaneously (heating: 1 h; cooling: 40 min), with only 1 operation per day in one year. Regarding the use of solar thermal energy, the collector area was considered 16 m^2 as reported for other similar systems (Mohanraj et. al., 2018) (Mostafa et. al. 2022).

In this way, the emission of $CO_{2(eq)}$ in the new system is based on the supply of thermal energy to provide the heating demand (11.58 kW), so that about 52% comes from the electrical heater inside the Storage tank (4.27 kW) and 48% from the solar thermal system (3.93 kW). Whereas the solar system must operate during the entire process time (2 h) in a year.

Table 2. Evaluation of the GWP between the proposed system and conventional systems.

Item	Description	Consumption kWh	CF	Total kg $CO_{2(eq)}$
1	Wood boiler	10,692.6	0.531	5,677.8
2	Refrigeration system	252.0	0.230	1,487.9 (57.9+1,430)
		GWP (R134a)	-	
3	Gas boiler	9,727.2	0.314	3,054.3
4	DCHP	6,285.3	0.230	2,879.6 (1,445.6+1,430+4)
		GWP (R134a + R600a)	-	
5	SAHP + SAACS	2,033.0	0.230	1,259.6 (467.6+4+30.7+40.4+716.9)
		GWP (R600a)	-	
		133.9	0.230	
		2,868.9	0.0141	
		3,117.1	0.230	

(1)CF: Carbon footprint (kg $CO_{2(eq)}$/kWh)

Therefore, it can be assessed that the implementation of the hybrid system (SAHP+SAACS) to meet the demands of heating and cooling effectively contributes to the reduction of about 3,282.6kg $CO_{2(eq)}$ per year (decrease of 72.2%) in relation to the conventional cooling system and gas boiler, about 5,906.1kg $CO_{2(eq)}$ per year (decrease of 82.4%) in relation to the conventional cooling system and wood boiler, and about 1,620.0kg $CO_{2(eq)}$ per year (decrease of 56.2%) in relation to the DCHP system.

4. CONCLUSION

The application of renewable energies to improve industrial manufacturing operations is motivated not only by the potential decarbonization of the sector but also by the desire to maintain a high degree of quality of its products while operating at the highest possible production rates in a sustainable way. Thus, in order to meet the demands of steam generation and cooled water typical of an industrial process, this study addressed simulations of the SAHP system, operating with R600a, integrated into a SAACS system, operating with the silica-gel/water pair, investigating its technical and environmental feasibility of application in a dry tropical savanna climate.

The simulations showed that such demands can be met, since the auxiliary thermal energy generation system is sized to meet the silica-gel regeneration temperatures in the ACS and condensation above 100°C in the HP. In addition, the hybrid system (SAHP+SAACS) obtained the lowest environmental impact, since its FC was lower compared to the other technologies studied (wood and gas boilers together with the cooling system and the systems with the DCHP). Thus, the study of the hybrid system is a favorable alternative when it is desired to reconcile the reduction of energy and environmental costs within the industrial processes of steam and cold-water generation.

5. ACKNOWLEDGEMENTS

The authors acknowledge the financial support given by the Coordenação de Aperfeiçoamento de Pessoal de Nível Superior - CAPES, and the Institute of Technological Innovation of the University of Pernambuco - IIT-UPE. Also, the authors would like to thank the Pernambuco Institute of Technology - ITEP for the technical support.

6. REFERENCES

ABNT NBR ISO 14044:2009, Versão Corrigida 2014 – Gestão ambiental, Avaliação do Ciclo de Vida, Requisitos e orientações – Publicada em 21.07.2014.

Alahmer, A., Wang, X., Al-Rbaihat, R., Alam, K. A., Saha, B. B., 2016. "Performance evaluation of a solar adsorption chiller under different climatic conditions". *Applied Energy*, Vol. 175, pp. 293-304.

Alfa Laval Aalborg, 2022. "Poder Calorífico Inferior". <https://bit.ly/3zKrL8 >.

Bawazir, A. A., Friedrich, D., 2022. "Evaluation and design of large-scale solar adsorption cooling systems based on energetic, economic and environmental performance". Energies, Vol. 15, pp. 2149.

Bellos, E., Tzivanidis, C., & Antonopoulos, K. A., 2016. "Exergetic and energetic comparison of LiCl-H2O and LiBr-H2O working pairs in a solar absorption cooling system". Energy Conversion and Management, Vol. 123, pp. 453-461.

Bernier, Nicolas, Bruno Marcotte, and Michaël Kummert, 2022. "Calling Python from TRNSYS with CFFI". Polytechnique Montréal. DOI: 10.5281/zenodo.6523078.

Cabrera, F. J., Fernández-García, A., Silva, R. M. P., & Pérez-García, M., 2013. "Use of parabolic trough solar collectors for solar refrigeration and air-conditioning applications". Renewable and sustainable energy reviews, Vol. 20, pp. 103-118.

Calise, F., Figaj, R. D., Vanoli, L., 2017. "A novel polygeneration system integrating photovoltaic/thermal collectors, solar assisted heat pump, adsorption chiller and electrical energy storage: Dynamic and energy-economic analysis". Energy Conversion and Management, Vol. 149, pp. 798-814.

Chandrasekaran, S. R., Laing, J. R., Holsen, T. M., Raja, S., and Hopke, P. K., 2011. "Emission characterization and efficiency measurements of high-efficiency wood boilers. *Energy & fuels*, Vol. 25, n. 11, pp. 5015-5021.

Chen, H., Li, Z., Xu, Y., 2019. "Evaluation and comparison of solar trigeneration systems based on photovoltaic thermal collectors for subtropical climates". *Energy Conversion and Management*, Vol. 199, pp. 111959.

Chen, H., Li, Z., Xu, Y., 2020. "Assessment and parametric analysis of solar trigeneration system integrating photovoltaic thermal collectors with thermal energy storage under time-of-use electricity pricing". *Solar Energy*, Vol. 206, pp. 875-899.

Dadpour, D., Deymi-Dashtebayaz, M., Hoseini-Modaghegh, A., Abbaszadeh-Bajgiran, M., Soltaniyan, S., Tayyeban, E., 2022. "Proposing a new method for waste heat recovery from the internal combustion engine for the double-effect direct-fired absorption chiller". Applied Thermal Engineering, Vol. 216, pp.119114.

Denzinger, C., Berkemeier, G., Winter, O., Worsham, M., Labrador, C., Willard, K., ... & Choi, J. K., 2021. "Toward sustainable refrigeration systems: Life cycle assessment of a bench-scale solar-thermal adsorption refrigerator". International Journal of Refrigeration, Vol. 121, pp. 105-113.

Dumbliauskaite, M., Becker, H., & Maréchal, F., 2010. "Utility optimization in a brewery process based on energy integration methodology". In Proceedings of the 23th International Conference on Efficiency, Cost, Optimization, Simulation and Environmental Impact of Energy Systems (No. CONF, pp. 91-98).

Embraco, 2020. "Guide for the use of HCs refrigerants R600a and R290". <https://bit.ly/3aSJzUg>.

Gado, M. G., Megahed, T. F., Ookawara, S., Nada, S., El-Sharkawy, I. I., 2021. "Performance and economic analysis of solar-powered adsorption-based hybrid cooling systems". Energy Conversion and Management, Vol. 238, pp. 114134.

Gado, M. G., Megahed, T. F., Ookawara, S., Nada, S., El-Sharkawy, I. I., 2022. "Potential application of cascade adsorption-vapor compression refrigeration system powered by photovoltaic/thermal collectors". Applied Thermal Engineering, Vol. 207, pp. 118075.

Guimarães, L. B., da Silva Guerra, I. G., da Silva, A. G., de Sousa, M. H., Lemos, V. F., Dutra, E. D., & Gómez-Malagón, L. A., 2022. "Potencial da energia solar térmica e fotovoltaica no setor de laticínios". In: Congresso Brasileiro de Energia Solar – CBENS, pp. 1-10.

Guimarães L. B., Dutra E. D., Gómez-Malagón L. A., 2022. "Performance Analysis of Double Cascade Heat Pump For Industrial Steam Generation". In Proceedings of the 19th Brazilian Congress of Thermal Sciences and Engineering – ENCIT 2022. Bento Gonçalves - RS, Brazil.

Haywood, A., Sherbeck, J., Phelan, P., Varsamopoulos, G., Gupta, S. K., 2012. "Thermodynamic feasibility of harvesting data center waste heat to drive an absorption chiller". Energy Conversion and Management, Vol. 58, pp. 26-34.

Hawlader, M. N. A., Chou, S. K., Ullah, M. Z. (2001). "The performance of a solar assisted heat pump water heating system". Applied thermal engineering, Vol. 21, pp.1049-1065.

Herrando, M., Simón, R., Guedea, I., Fueyo, N., 2021. "The challenges of solar hybrid PVT systems in the food processing industry". Applied Thermal Engineering, Vol. 184, pp. 116235.

Hiben, Y. G., Bayray, M., Lauwaert, J., 2023. "Optimizing solar-assisted industrial heating and cooling system for cost-effective installation". Applied Thermal Engineering, Vol. 230, pp. 120778.

Huijbregts, M. A., Steinmann, Z. J., Elshout, P. M., Stam, G., Verones, F., Vieira, M., Zijp, M., Hollander, A., Van Zelm, R., 2017. "ReCiPe2016: a harmonized life cycle impact assessment method at midpoint and endpoint level". The International Journal of Life Cycle Assessment, Vol. 22, n. 2, pp. 138-147.

IDEC, 2022. "Emenda de Kigali: benefícios de sua ratificação pelo Congresso Nacional". <https://bit.ly/3n17mUO>.

IPCC, 2023. "Summary for Policymakers". Climate Change 2023: Synthesis Report. Contribution of Working Groups I, II and III to the Sixth Assessment Report of the Intergovernmental Panel on Climate Change [Core Writing Team, H. Lee and J. Romero (eds.)]. IPCC, Geneva, Switzerland, pp. 1-34, doi: 10.59327/IPCC/AR6-9789291691647.001.

Jiang, J., Hu, B., Wang, R. Z., Deng, N., Cao, F., and Wang, C. C., 2022. "A review and perspective on industry high-temperature heat pumps". *Renewable and Sustainable Energy Reviews*, Vol. 161, pp. 112106.

Jugjai, S., Rungsimuntuchart N., 2002. "High efficiency heat-recirculating domestic gas burners". *Experimental thermal and Fluid Science*, Vol. 26, n. 5, pp. 581-592.

Kang D. H., Na S., Kim M. S., 2017. "Recent Research on Steam Generation Heat Pump System". International Journal of Air-Conditioning and Refrigeration, Vol. 25, pp. 1730005.

Li, H., Sun, L., Zhang, Y., 2014. "Performance investigation of a combined solar thermal heat pump heating system". Applied Thermal Engineering, Vol. 71, pp. 460-468.

Liu, Y., Groll, E. A., Yazawa, K., & Kurtulus, O., 2017. "Energy-saving performance and economics of CO2 and NH3 heat pumps with simultaneous cooling and heating applications in food processing: Case studies". International Journal of Refrigeration, Vol. 73, pp. 111-124.

Lin Y., Xu H., Shan X., Di Y., Zhao A., Hu Y., Gan Z., 2019. "Solar steam generation based on the photothermal effect: from designs to applications, and beyond". Journal of Materials Chemistry A, Vol. 7, pp. 19203 – 19227.

Liu, Z., Xie, N., & Yang, S., 2020. "Thermodynamic and parametric analysis of a coupled LiBr/H2O absorption chiller/Kalina cycle for cascade utilization of low-grade waste heat". Energy Conversion and Management, Vol. 205, pp. 112370.

Lu Z., Yao Y., Liu G., Ma W., Gon Y., 2022. "Thermodynamic and Economic Analysis of a High Temperature Cascade Heat Pump System for Steam Generation". Processes, Vol. 10, pp. 1862.

Lu, Z. S., Wang, R. Z., Xia, Z. Z., Wu, Q. B., Sun, Y. M., & Chen, Z. Y. (2011). "An analysis of the performance of a novel solar silica gel–water adsorption air conditioning". Applied Thermal Engineering, Vol. 31, pp. 17-18.

Mateu-Royo C., Arpagaus C., Mota-Babiloni A., Navarro-Esbrí J., Bertsch S. S., 2021. "Advanced high temperature heat pump configurations using low GWP refrigerants for industrial waste heat recovery: A comprehensive study". Energy Conversion and Management, Vol. 229, pp. 113752.

Masera, K., Tannous, H., Stojceska, V., & Tassou, S., 2023. "An investigation of the recent advances of the integration of solar thermal energy systems to the dairy processes". Renewable and Sustainable Energy Reviews, Vol. 172, pp. 113028.

MinData, 2023. "Köppen climate type located". <https://www.mindat.org/feature-3399058.html>.

Mohanraj, M., Belyayev, Y., Jayaraj, S., & Kaltayev, A., 2018. "Research and developments on solar assisted compression heat pump systems–A comprehensive review (Part-B: Applications)". *Renewable and Sustainable Energy Reviews*, Vol. 83, pp. 124-155.

Mostafa, A., Hassanain, M., & Elgendy, E., 2022. "Transient simulation and design parameters optimization of a cold store utilizes solar assisted adsorption refrigeration system". *Case Studies in Thermal Engineering*, Vol. 37, pp. 102273.

Mueller, Stefan C.; Remund, Jan; Meteotest, A. "Validation of the Meteonorm satellite irradiation dataset". Proceedings of the 35th European Photovoltaic Solar Energy Conference and Exhibition, Brussels, Belgium. 2018. p. 24-27.

Najeh, G., Slimane, G., Souad, M., & Riad, B., 2016. "Performance of silica gel-water solar adsorption cooling system". Case Studies in Thermal Engineering, Vol. 8, pp. 337-345.

Saini, P., Ghasemi, M., Arpagaus C., Bless F., Bertsch S., Zhang X., 2023. "Techno-economic comparative analysis of solar thermal collectors and high-temperature heat pumps for industrial steam generation". Energy Conversion and Management, Vol. 277, pp. 116623.

Younes, M. B., Shaban, N. A., Altork, Y., 2023. "Modelling and performance assessment of a Tri–Generation cooling system using two adsorption chillers under Jordanian climate". Case Studies in Thermal Engineering, Vol. 44, pp. 102848.

Wu Z., Wang X., Sha L., Li X., Yang X., Ma X., Zhang Y., 2021. "Performance analysis and multi-objective optimization of the high-temperature cascade heat pump system". Energy, Vol. 223, pp. 120097.

7. RESPONSIBILITY NOTICE

The authors are the only responsible for the printed material included in this paper.